Development of very large helicon plasma source

Shunjiro Shinohara[a)]
Interdisciplinary Graduate School of Engineering Sciences, Kyushu University, Kasuga, Fukuoka 816-8580, Japan

Takao Tanikawa
Research Institute of Science and Technology, Tokai University, Shibuya-ku, Tokyo 151-8677, Japan

(Received 23 September 2003; accepted 23 February 2004; published online 21 May 2004)

We have developed a very large volume, high-density helicon plasma source, 75 cm in diameter and 486 cm in axial length; full width at half maximum of the plasma density is up to ~42 cm with good plasma uniformity along the *z* axis. By the use of a spiral antenna located just outside the end of the vacuum chamber through a quartz-glass window, plasma can be initiated with a very low value of radio frequency (rf) power (<1 W), and an electron density of more than $10^{12}\,\mathrm{cm}^{-3}$ is successfully produced with less than several hundred Watt; achieving excellent discharge efficiency. It is possible to control the radial density profile in this device by changing the magnetic field configurations near the antenna and/or the antenna radiation-field patterns. © *2004 American Institute of Physics.*
[DOI: 10.1063/1.1753089]

I. INTRODUCTION

In various plasma-related fields, such as plasma processing, fusion, and basic fields including the study of space plasmas, it is crucial to construct a large volume, high-density plasma source. Additionally, profile control under various magnetic field configurations is an important requirement. A helicon wave plasma source[1–6] is expected to be a promising source that could satisfy the above-noted requirements, and is attracting a growing interest for various applications and in basic plasma research. Recently, an application to a magnetoplasma rocket[7] utilizing this wave was proposed. Here, the helicon wave is a bounded electromagnetic wave in the whistler wave range of frequencies (between the ion and electron cyclotron frequencies) with both right- and left-handed circular polarizations.

High-density helicon plasma is usually produced in a small insulator tube (its inner radius is typically less than 10 cm) immersed in a uniform magnetic field using an antenna that consists of metal strips wound around the outside of the tube (e.g., Fig. 5 in Ref. 3). Few attempts have been made to produce larger diameter helicon plasma, except for the experiment performed at Kyushu University[8,9] with a vacuum vessel of 45 cm in diameter and 170 cm in axial length using a spiral antenna. This type of spiral antenna has been used in inductively coupled plasma,[10] and as far as we know, apart from our experiments, there is only one experiment using this type of the antenna to produce helicon plasma: this being in a density range of 10^{11}–$10^{12}\,\mathrm{cm}^{-3}$ using a short chamber of 25 cm long and 48 cm in diameter under a weak field.[11]

In this article, we describe the development of a very efficient, large-volume helicon plasma source (75 cm in diameter and 486 cm in axial length) at the Institute of Space and Astronautical Science (ISAS) of Japan, the Japan Aerospace Exploration Agency (JAXA). With this, plasma can be initiated with a very low value of radio frequency (rf) power (<1 W), and an electron density of more than $10^{12}\,\mathrm{cm}^{-3}$ is successfully produced with less than several hundred watts. Note that to our knowledge the plasma volume in this source of up to 2.1 m^3 is the largest using a helicon wave (see Table I). In this new device, we again employ a spiral antenna scheme and consider some constraints such as trials to decrease (increase) an inductance (plasma-coupling) of a large size antenna. Here, we aimed to produce large helicon plasma with high efficiency, as well as controlling the radial density profile by two methods: (1) by changing the magnetic field configurations and (2) by changing the antenna radiation-field patterns. Therefore, our large source with the capability of controlling the plasma profile could be expected to extend opportunities in the plasma processing field by making available a large-diameter, high density plasma in a low fill pressure condition, and also contribute to fundamental studies of fusion and space plasmas that inevitably require a large volume.

Table I shows a comparison of large helicon sources from different organizations.[8,9,12–20] Even though some of the machine sizes (excluding our cases) are relatively large, the actual diameter of the produced plasmas are much smaller than the device diameter in spite of utilizing some innovative techniques, e.g., multi-helicon-sources located at the end of the chamber (New Mexico Tech.)[21] and the use of an internal loop antenna inside a chamber (Max Planck Institute, Greifswald).[22] The machines at West Virginia and Ruhr Universities consist of two sections: the helicon plasma source and the diffusion chamber, whose size is much larger than the former section. In this configuration, the plasma produced flows into the diffusion region in which the background magnetic field strength is much weaker than that in the source region, resulting in a lower-density plasma in the diffusion region than in the source region.

Several advantages of using a spiral antenna are: (1) The

a)Electronic mail: sinohara@aees.kyushu-u.ac.jp

TABLE I. Comparison of sizes between various large helicon sources reported by different organizations. Rough estimations have been done as to the production efficiency N_e/P_{rf}, with the typical conditions of axial magnetic field and a fill pressure. Here, N_e and P_{rf} are total number of electrons and input rf power, respectively.

Organization	Machine size (diameter, length) in cm	N_e/P_{rf} in 10^{13} (l/W)	Remarks
ISAS/JAXA	(75,486) (Present)	~100 (0.14 kG, 2 mTorr)	Spiral antenna
Kyushu Univ.	(45,170) (Refs. 8 and 9)	~30 (<0.2 kG, 10 mTorr)	Spiral antenna
New Mexico Tech.	(43,400) (ALPHA) (Ref. 12)	~8 (0.8 kG, 3 mTorr)	Smaller plasma diameter than device diameter; antenna array
Max Planck Institute (Greifswald)	(40,400) (VINETA) (Refs. 13 and 14)	~2 (0.85 kG, 2 mTorr)	Smaller plasma diameter than device diameter
Univ. California, San Diego	(20,250) (CSDX) (Ref. 15)	~0.7 (a few mTorr)	Smaller plasma diameter than device diameter
Australian National Univ.	(20,50)+(90,250) (Ref. 16)	~2 (0.1 kG, 3 mTorr)	Weak field
Auburn Univ.	(17,250) (ALEPSI) (Ref. 17)	~5 (0.8 kG, 9 mTorr)	Smaller plasma diameter than device diameter
Ruhr Univ.	(15,200) +(60,100) (Ref. 18)	~5 (<1 kG)	Multipole (weak) field in large diameter chamber
West Virginia Univ.	(15,157) (HELIX)+(200, 450) (LEIA) (Refs. 19 and 20)	~5 (<1 kG, 6 mTorr)	Weak field in LEIA

antenna can be located outside the vacuum vessel. In practice, it only needs to be positioned just outside an inexpensive insulator window at the end of the vessel. (2) As a result, the antenna can be easily installed or removed as necessary. (3) An impedance matching circuitry (in a match box) can easily be set up just behind the antenna, reducing the adverse inductive effect. (4) The plasma production can be initiated at very low rf power due to the good initial capacitive coupling. (5) The antenna radiation pattern can be easily varied by changing the rf feed points on the antenna. This method can be used to control the radial plasma density profile described in more detail in Sec. III.

This article is organized as follows. Section II describes in detail our experimental setup to produce large-volume plasma, utilizing two types of spiral antennae. Experimental results, including examples of the plasma density as a function of the input radio frequency (rf) power, and some examples of control of the radial density profile by changing the magnetic field configurations and the antenna radiation field patterns, are briefly presented in Sec. III.

II. EXPERIMENTAL SETUP

Our experiments at ISAS/JAXA are performed in a vacuum chamber, 75 cm and 73.8 cm in outer diameter (o.d.) and inner diameter (i.d.), respectively, and 486 cm in axial length [see Fig. 1(a)]. Here, the 14 main coils produce a uniform magnetic field in the central region (over 2 m in the axial direction [see Fig. 2(a)]). The main coil current of $I_m = 50$ A corresponds to 140 G. Due to the lack of coils at both ends of the machine, the magnetic field is weaker (nonuniform field) in these regions. To compensate for the weak magnetic field near the spiral antenna located at one end of the chamber, separate coils are additionally installed [see the right-hand side of the chamber in Fig. 1(a)] and an independent power supply is used for these coils. Here, the separate coil current $I_s = 0$, 10, and 20 A corresponds to the axial magnetic field near the antenna $B_a = 11$, 30, and 50 G, respectively, with $I_m = 50$ A. Note that the separate coil current, I_s, does not significantly alter the main central field generated by I_m. Figure 2 shows three cases of a magnetic flux function under the above-noted conditions; indicating that a weaker convergent field is formed with an increase in I_s (the magnetic field near the antenna, i.e., $z \sim 0$ cm, becomes more uniform as I_s is increased). Here, $z = 0$ cm corresponds to the vacuum side surface of the quartz-glass window. As is described later in Sec. III, it is possible to control the radial density profile by changing the magnetic field pro-

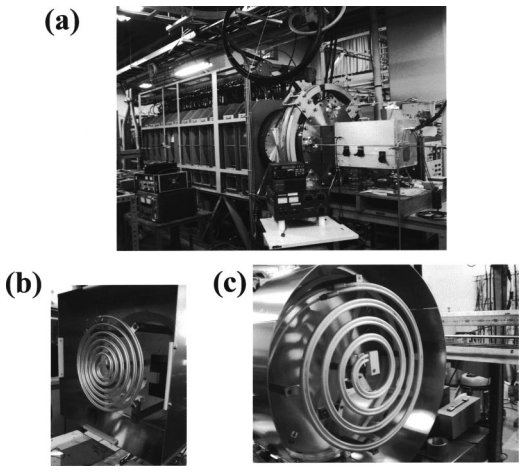

FIG. 1. (a) A large volume plasma source attached to an impedance match box through a spiral antenna, and (b) small (type A) and (c) large (type B) spiral antennae.

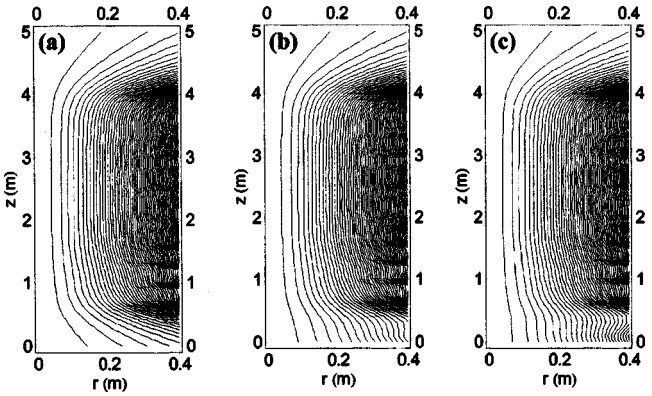

FIG. 2. Contour plots of the calculated magnetic flux functions, changing the separate coil current I_s near the antenna, with the main field of 140 G (main coil current $I_m=50$ A): $I_s=$(a) 0 A, (b) 10 A, and (c) 20 A.

file near the antenna (by changing the coil current I_s near the antenna). The base pressure of our device is $\sim 10^{-7}$ Torr using a turbomolecular pump at a pumping speed of 1800 l/s [the right bottom side of the chamber in Fig. 1(a): not seen], and the typical working gas through a needle valve (the left side of the chamber: not seen) is argon (Ar) with a fill pressure, P_{Ar}, of 0.2–2 mTorr.

Next, the rf system used in our experiment is described. Two different sizes of spiral antennae are used: the smaller one [type A: Fig. 1(b)] has 6 turns and a 23 cm o.d., and the larger one [type B: Fig. 1(c)] has 4 turns and a 43 cm o.d. Each has taps for electrical connections at every half turn (they cannot be seen clearly in Fig. 1). Any of two connection points on each antenna can be chosen to feed the rf power in order to easily enable variation of the antenna radiation pattern. This in turn causes a change in the plasma production process, making it possible to control the radial plasma density profile as described in Sec. III. Two pieces of copper (Cu) tubing are used to construct a spiral antenna to provide the inlet and outlet for cooling water; they are spiraled side by side and joined at a central position of the antenna structure.

In type A, 0.6 cm o.d. Cu tubing is used, and two pieces are positioned with the same radial position, i.e., two adjacent layers in the axial direction. On the other hand, two pieces of 1 cm o.d. Cu tubing are placed in the same plane for type B. The antenna vacuum inductance L_v and vacuum resistance R_v of type A (type B) without plasma are $\sim$4.6 μH ($\sim$5.1 μH) and $\sim$0.85 Ω ($\sim$0.85 Ω), respectively, including the feed lines in the match box, at a frequency of 7 MHz. Note that the inductances of type A and type B antennae with the spiral part only are $\sim$2.8 and $\sim$3.3 μH, respectively. Here, the high-voltage rf feeding point is at the outside edge of the antenna and the ground point is at its center. The reverse of the feeding points changes the above values by less than 10%. We note here that the antenna inductance should be kept low for easy impedance matching between the antenna and the transmitter, especially for higher excitation frequency cases, and also should be kept low to achieve low antenna voltage operation. For this reason, the number of spiral turns for the larger antenna is smaller than that of the smaller one. As a result, the impedance of the type B antenna is not appreciably larger than that of the type A one. Although the cross section of Cu tubing used for type B is also larger than that for type A, it did not significantly decrease the antenna inductance.

These antennae are located outside the vacuum chamber, in the atmosphere at a quartz-glass window. The diameter and thickness of the quartz window for type A (type B) antenna are 30 cm (52 cm) and 1.6 cm (3 cm), respectively. The distance between the surfaces of the quartz-glass window and the antenna is 0.5–1 cm. For the type B antenna, there are several cutouts along the axial direction on a cylindrical antenna cover of 58.1 cm o.d. to reduce the rf eddy currents of the metal cover, so that the problems of inducing the eddy current and metal heat-up can be eliminated.

In the match box [on the right-hand side of Fig. 1(a)] with a square cross section of 40 cm$\times$40 cm, and 60 cm in axial direction, a split tank circuit is employed: in series and parallel connections, vacuum variable capacitors of 1500 pF (2 pieces) and 2000 pF are used. To meet the impedance matching requirement in a wide range of excitation frequencies with and without plasma, 12 fixed-valued capacitors of 1200–1500 pF can be installed in the box, as of necessity. Forward and reflected rf power, P_{for} and P_{ref}, respectively, are monitored using a directional coupler, and the rf input power P_{inp} to the plasma source is defined as $P_{\mathrm{for}}-P_{\mathrm{ref}}$. The antenna rf current and voltage are measured by a current monitor with a fast time response [Model 6600 (Pearson Electronics, Inc.)] and by a series connection point of capacitances, respectively. In our experiments, the maximum output power of the rf amplifier [A60-6601 (Thamway Co., Ltd.)] is 1 kW at a typical frequency of 7 MHz. Both continuous (cw) and pulsed mode (a typical pulse width is 40 ms with a duty-cycle of 0.04) operations are used.

The spatial plasma parameters, such as plasma density and electron temperature (typically 3–5 eV), are measured by scanning three Langmuir probes (one-sided tantalum disk probes of 0.2–0.5 cm in diameter). Two probes are inserted from the ends of the chamber, so that they can move along the axial direction. The third probe, which can move radially, is inserted radially into the chamber at the axial position of $z=150$ cm. The excited rf wave field patterns are measured by two one-turn magnetic probes, of $\sim$1 cm in diameter constructed from semirigid coaxial cables; one can move along the axial direction from the right end flange, and the other can move radially at $z=150$ cm. These Langmuir and magnetic probes inserted from both end flanges can be rotated to measure the radial profiles as well, since the top section of each probe is bent by 90° with respect to the chamber axis. Ordinary digital cameras are used to monitor the plasma light. Observation windows are provided on the end flanges of both sides of the chamber and on the side of the chamber at $z=31.5$ cm.

III. EXPERIMENTAL RESULTS

Figure 3 shows the plasma density n_e as a function of the input rf power P_{inp}, using the type B antenna. Plasma production can be initiated at a P_{inp} of very low value ($<$1 W). A low-density region of the order of 10^9 cm^{-3} can be

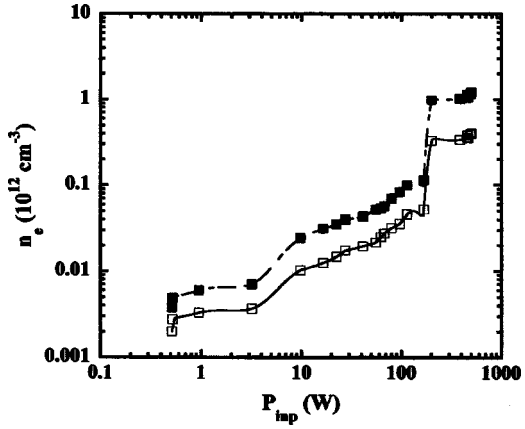

FIG. 3. Electron density n_e as a function of the input rf power P_{inp}, using the large spiral antenna (type B) with a fill pressure of $P_{\mathrm{Ar}}=2$ mTorr. Here, the main field is 140 G (the main current $I_m=50$ A), with the separate coil current $I_s=15$ A, and the open (closed) boxes show the data points taken at $z=40$ (150) cm.

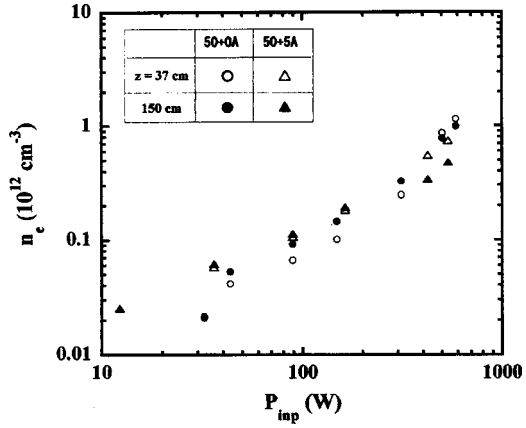

FIG. 4. Electron density n_e as a function of the input rf power P_{inp}, using the large spiral antenna (type B) with a fill pressure of $P_{\mathrm{He}}=0.75$ mTorr. Here, the main field is 140 G with the main coil current $I_m=50$ A, and the open and closed circles (open and closed triangles) show the data points taken at $z=40$ and 150 cm, respectively, with the separate coil current I_s of 0 A (5 A).

considered as a region in a capacitively coupled plasma (CCP) discharge. As P_{inp} increases, the density n_e rises to a higher order of $10^{10}\,\mathrm{cm}^{-3}$ [CCP and/or inductively coupled plasma (ICP), which mechanism is dominant cannot be clearly determined though an ICP effect can be stronger in a higher density region]; then, a density jump, known as a mode change from ICP to helicon plasma discharges,[23] is observed at $P_{\mathrm{inp}}\sim 200\,\mathrm{W}$. We have verified the helicon discharge by identifying the helicon dispersion relation and the radial profile of excited waves by measuring the axial component of the rf magnetic field (not shown). This density jump is clearer for the stronger magnetic field near the antenna (by increasing I_s); at the same time the threshold input power for the jump increases.

As can be seen in Table I, the production efficiency of N_e/P_{rf}, which shows the ratio of total number of electrons to input rf power, is very high in our machine compared to the other machines by more than one order of magnitude, except for the experiment at Kyushu University. Note that these values are estimated very roughly using some assumptions such as density profile, and they do not always show typical values due to the limitations of using published data. This ratio of N_e/P_{rf} also means the electron density per unit rf power density, and it is proportional to the (kinetic) energy confinement time τ_e. From the data in Table I, N_e/P_{rf} scales roughly with the plasma cross section (not shown).

Using both types A and B antennae, plasma production can be initiated with an input rf power of <1 W, regardless of the magnetic field strength (from 0 to 1600 G) and of a fill pressure over 0.2 mTorr (plasma can be produced at >2 mTorr; however, the pumping condition must be taken into account). The position of the maximum plasma density in the axial direction lies between $z\sim 60\,\mathrm{cm}$ and $z\sim 150\,\mathrm{cm}$, depending on the experimental conditions, such as a fill pressure and the magnetic field geometry (degree of convergent field). The plasma uniformity along the z axis is very good; the decay length after the maximum density position is typically >100 cm. This length becomes even longer with a decrease in fill pressure and an increase in the separate coil current I_s (weaker convergent field).

As for the antenna–plasma coupling, the total antenna loading R_t, which is the sum of R_v and R_p (plasma loading), increases abruptly after the density jump, and R_t is a factor 3–10 larger than R_v, i.e., a very good coupling due to the high density. There is a tendency that this factor increases with an increase in I_m (the main field) and a decrease in I_s (the field near the antenna). The discharge for helium (He) gas is quite similar to that in the case of Ar, contrary to the expectation that He plasma generally needs much more rf power to have high density. A plasma density of $n_e > 10^{12}\,\mathrm{cm}^{-3}$ can be achieved at $P_{\mathrm{inp}}>500\,\mathrm{W}$ for $I_{\mathrm{m}}=50\,\mathrm{A}$, $I_s=0\,\mathrm{A}$, and a He fill pressure of $P_{\mathrm{He}}=0.75\,\mathrm{mTorr}$, as is shown in Fig. 4. It is difficult to initiate the plasma with $P_{\mathrm{He}}<0.3\,\mathrm{mTorr}$, but with an introduction of electron supply using a small heated tungsten wire, the operating pressure in the low pressure region becomes wider.

Finally, we describe the control of the radial density profile by varying the magnetic field profile near the antenna, or the antenna radiation field pattern. The former is attained by adjusting the separate coil current I_s near the antenna, while the latter is attained by changing the rf feeding positions on the antenna. Figure 5 shows an example of the former method. Three photos were taken from the observation port in the neighborhood of the antenna [the right flange in Fig. 1(a)], changing the separate coil current I_s near type A antenna. Due to the perspective effect, the plasma diameter seems to diminish very quickly along the axial direction; however, the actual plasma column diameter stays nearly constant along the z axis. It can be seen that the plasma light extends to the other end of the chamber along the axis (see the right side of the bright part in each photo), and with the increase in the magnetic field near the antenna (the increase in I_s), the plasma column becomes broader [see the bright part from Figs. 5(a) to 5(c)]. This is ascertained by radial profile measurements of the ion saturation current at $z=150\,\mathrm{cm}$, where the full width at half maximum (FWHM) increases from 18 to 22 cm (see Fig. 6). This tendency can be

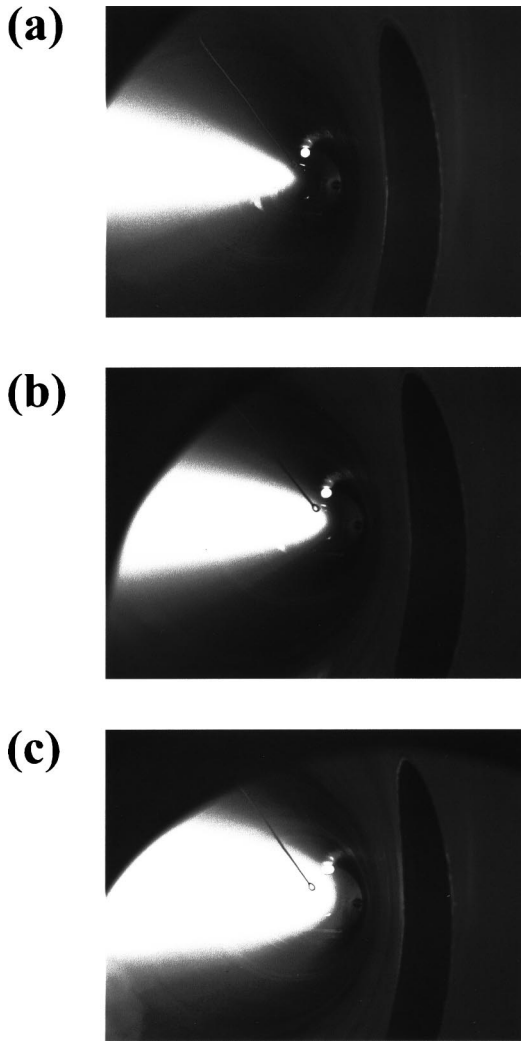

FIG. 5. Photos taken from the observation port in the neighborhood of the antenna, changing the separate coil current I_s near the small antenna (type A), with the main field of 140 G (main coil current $I_m = 50$ A) and a pressure of $P_{\mathrm{Ar}} = 2$ mTorr. The separate coil current I_s and input rf power P_{inp} are (a) 0 A and 523 W, (b) 10 A and 257 W, and (c) 15 A and 398 W, respectively. The probe structure hung from the upper left is a one-turn magnetic loop, and the skewed oval shape (in black) on the right-hand side is an access port in the vacuum vessel.

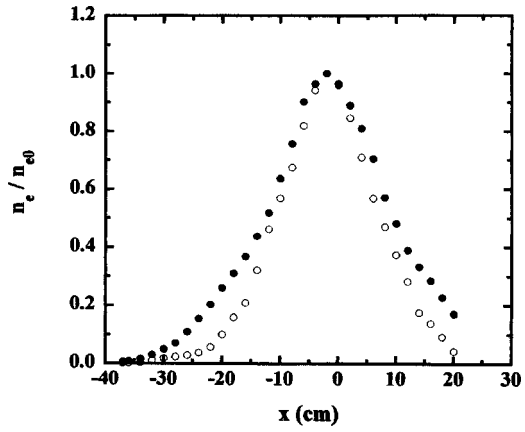

FIG. 6. Radial profiles of the normalized electron density $n_e(r)/n_{e0}$ with a pressure of $P_{\mathrm{Ar}} = 2$ mTorr. Here, the maximum electron density n_{e0}, input rf power P_{inp}, the main coil current I_m, and the separate coil current I_s near the type A antenna for the open (closed) circles are 1.2 (1.7) $\times 10^{12}$ cm^{-3}, 600 (350) W, 50 (50) A, and 0 (15) A, respectively.

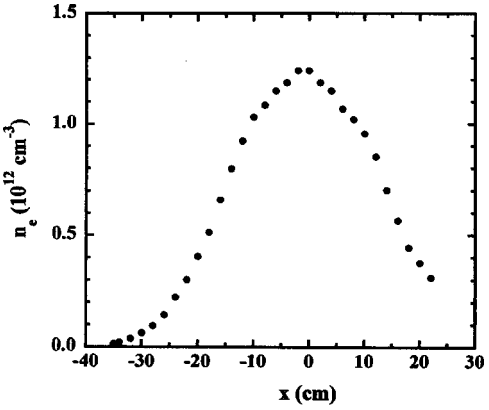

FIG. 7. Radial profiles of the normalized electron density n_e with a pressure of $P_{\mathrm{Ar}} = 2$ mTorr. Here, the input power P_{inp}, main coil current I_m, and separate coil current I_s near the type B antenna are 412 W, 50 A, and 16 A, respectively.

understood from the magnetic field configurations: the weaker convergent field with the increase in I_s makes the density profile broader due to the plasma flow and the wave propagation along the field. Needless to say, as shown in Fig. 7, the radial density profile becomes much broader (FWHM is 32 cm) with the use of a larger spiral antenna (type B) compared to a smaller one (type A).

The effectiveness of the second method of controlling the radial density profile by changing the antenna radiation field pattern is tested by comparing between the results obtained using the inner two turns and the outer two turns of the type B spiral antenna as a radiation source. When the outer two turns are used as a radiation source, the radial density profile is somewhat hollow shaped (i.e., there is a shallow dip at the center) and is broader than the profile obtained using the inner two turns. This is a reflection of the change of the antenna's radiated field pattern. We have succeeded in expanding the plasma radial size (FWHM) with up to ~42 cm using the higher I_s value and/or the use of the outer two turns of the spiral antenna.

It has also been found that even if the same inner two turns are used, the radial density profile can be quite different depending upon which position the antenna feed point is grounded or connected to on the high-voltage side. The profile shows a broader, somewhat hollow shape when the high-voltage feeding point is connected to the outer position and the central position of the antenna is grounded; while the profile becomes peaked at the center when the central position is at a high-voltage and the outer position is grounded. This can be understood as a CCP generation effect, since the whole outer two-turn region is kept at a high-voltage when the high-voltage feeding point is connected to the outer position of the antenna.

ACKNOWLEDGMENTS

Our experiments have been carried out at ISAS/JAXA under their research collaboration program. Continuous encouragements from Professor Y. Nakamura, Professor Y. Kawai, and Professor K. Oyama have been greatly appreciated. We would also like to thank S. Sato, I. Funaki, and K.

Aihara for their help in carrying out the experiments. The research has been partially supported by Grants-in-Aid for Scientific Research (B)(2), Nos. 15340199 and 1435051, from the Japan Society for the Promotion of Science.

[1] R. W. Boswell, Phys. Lett. **33A**, 457 (1970).
[2] M. A. Lieberman and A. J. Lichtenberg, *Principles of Plasma Discharges and Materials Processing* (Wiley, New York, 1994).
[3] S. Shinohara, Jpn. J. Appl. Phys., Part 1 **36**, 4695 (1997), and references therein.
[4] R. W. Boswell and F. F. Chen, IEEE Trans. Plasma Sci. **25**, 1229 (1997), and references therein.
[5] F. F. Chen and R. W. Boswell, IEEE Trans. Plasma Sci. **25**, 1245 (1997), and references therein.
[6] S. Shinohara, J. Plasma Fusion Res. **78**, 5 (2002), and references therein [mostly in Japanese].
[7] F. R. Chang-Diáz, Res. Status Variable Specific Impulse Magnetoplasma Rocket **35**, 87 (1999).
[8] S. Shinohara, S. Takechi, and Y. Kawai, Jpn. J. Appl. Phys., Part 1 **35**, 4503 (1996).
[9] S. Shinohara, S. Takechi, N. Kaneda, and Y. Kawai, Plasma Phys. Controlled Fusion **39**, 1479 (1997).
[10] J. Hopwood, Plasma Sources Sci. Technol. **1**, 109 (1992).
[11] J. E. Stevens, M. J. Sowa, and J. L. Cecchi, J. Vac. Sci. Technol. A **13**, 2476 (1995).
[12] C. Watts, 43rd Annual Meetings of the Division of Plasma Physics, Long Beach, CA, 2000, Vol. 46, p. 32.
[13] C. M. Franck, O. Grulke, and T. Klinger, Phys. Plasmas **9**, 3254 (2002).
[14] C. M. Franck, O. Grulke, and T. Klinger, Phys. Plasmas **10**, 323 (2003).
[15] J. George, M. Burin, G. Tynan, and Seok-Min Yun, the 42nd Annual Meetings of the Division of Plasma Physics and the 10th International Congress on Plasma Phys., Quebec City, 2000, Vol. 45, p. 337.
[16] J. Scharer, A. Degeling, G. Borg, and R. Boswell, Phys. Plasmas **9**, 3734 (2002).
[17] J. Hana and C. Watts, Phys. Plasmas **8**, 4251 (2001).
[18] M. Krämer, B. Lorenz, and B. Clarenbach, Plasma Sources Sci. Technol. **11**, A120 (2002).
[19] P. A. Keiter, E. E. Scime, and M. Balkey, Phys. Plasmas **4**, 2741 (1997).
[20] M. W. Balkey, R. Boivin, J. L. Kline, and E. E. Scime, Plasma Sources Sci. Technol. **10**, 284 (2001).
[21] C. Watts, J. Allen, S. Hawkes, A. Searl, and S. B. Spores, the 44th Annual Meetings of the Division of Plasma Physics, Orlando, FL, 2002, Vol. 47, p. 32.
[22] C. M. Franck and T. Klinger, the 43rd Annual Meetings of the Division of Plasma Physics, Long Beach, CA, 2001, Vol. 46, p. 31.
[23] A. R. Ellingboe and R. W. Boswell, Phys. Plasmas **3**, 2797 (1996).